

Effect of low-level titanium(IV) doping on the resistivity of magnetite near the Verwey transition

Z. Kąkol,* J. Sabol,† J. Stickler,‡ and J. M. Honig

Department of Chemistry, Purdue University, West Lafayette, Indiana 47907-1393

(Received 16 October 1991)

The effects of Ti substitution for Fe on octahedral sites in magnetite has been investigated through electrical resistivity measurements. In a manner analogous to zinc ferrites, the Verwey transition temperature is depressed with increasing Ti content. The Verwey transition is of first order in $\text{Fe}_{3-y}\text{Ti}_y\text{O}_4$ in the concentration range $0 \leq y \leq y_c = 0.012$; for $y_c \leq y \leq 3y_c$ the transition is of second order, and for $y > 3y_c$ the phase transformation is completely eliminated. The data are correlated with comparable work on dilute zinc ferrites and nonstoichiometric magnetite, and the implications of the findings are discussed.

INTRODUCTION

Although the Verwey transition in magnetite has been extensively studied, many aspects of this phase transformation are not yet completely understood. It was recognized quite early that the transition temperature T_V was strongly affected by variations in oxygen stoichiometry¹⁻⁴ and by substitution of iron with other transition metal cations. These matters were not followed up further until their consideration was revived in more recent studies.⁵⁻¹¹ Detailed reports have been published recently on the changes in physical properties concomitant to alterations of the oxygen to iron ratio in $\text{Fe}_{3(1-\delta)}\text{O}_4$, or to the replacement of iron by zinc on tetrahedral cation sites to form $\text{Fe}_{3-x}\text{Zn}_x\text{O}_4$, or to the replacement of titanium on octahedral cation sites to form $\text{Fe}_{3-y}\text{Ti}_y\text{O}_4$.¹²⁻¹⁹ Through heat capacity measurements on magnetite it was demonstrated that in the range $-0.0005 < \delta < \delta_c = 0.0039$ the Verwey transition is of first order, whereas in the range $\delta_c \leq \delta \leq 3\delta_c$, the transformation is of higher order. This feature was independently verified by observation¹³ of discontinuities at T_V in the resistivity ρ and Seebeck coefficients α of specimens with $\delta \leq \delta_c$, whereas for $\delta > \delta_c$, ρ and α exhibited discontinuities in slope at temperatures close to T_V . Analogous observations of the electrical characteristics have been reported for the $\text{Fe}_{3-x}\text{Zn}_x\text{O}_4$ system.¹⁸ In both cases, and for both the first- and higher-order regimes, T_V decreases linearly with increasing cation vacancy density or with Zn substitution, with the correspondence $x = 3\delta$, as might be anticipated from the elementary comparison of $\text{Fe}_{3(1-\delta)}\text{O}_4$ with $\text{Fe}_{3-x}\text{Zn}_x\text{O}_4$: plots of T_V vs x and 3δ could be nearly superposed (see also Fig. 5 of the present paper).

For comparison purposes it appeared of interest to undertake studies of the $\text{Fe}_{3-y}\text{Ti}_y\text{O}_4$ system. As is well established, titanium replaces iron on octahedral interstices for $y < 0.2$, whereas zinc enters the lattice substitutionally on tetrahedral sites. When Ti^{4+} substitution occurs, charge balance requires the conversion of a corresponding amount of Fe^{3+} to Fe^{2+} . In the range $0 \leq y < 0.2$ the resulting titanomagnetite is characterized by the formula

$(\text{Fe}^{3+}) [\text{Fe}_{1+y}^{2+} \text{Fe}_{1-2y}^{3+} \text{Ti}_y^{4+}] \text{O}_4$, where the round and square brackets enclose ions located on tetrahedral and octahedral interstices, respectively. By contrast, dilute zinc ferrites are characterized by the formula $(\text{Zn}_x^{2+} \text{Fe}_{1-x}^{3+}) [\text{Fe}_{1-x}^{2+} \text{Fe}_{1+x}^{3+}] \text{O}_4$, showing that charge balance requires the conversion of Fe^{2+} to Fe^{3+} on octahedral sites.

A very elementary analysis²⁰ shows that when electron transport involves small polarons as charge carriers, the conductivity is given by $\sigma = A c v \mu$; in the present case A is a collection of parameters, c is the carrier density on octahedral sites (i.e., $[\text{Fe}^{2+}]$), v is the density of vacant octahedral sites (i.e., $[\text{Fe}^{3+}]$), and $\mu = \mu_0 \exp(-\epsilon_\sigma / k_B T)$ is the mobility, characterized by a conductivity activation energy ϵ_σ , k_B being the Boltzmann constant. In zeroth order, one may therefore anticipate that Ti^{4+} and Zn^{2+} substitutions should give rise to mirror image effects, so that the variation of σ with the Zn^{2+} or Ti^{4+} content of the sample should be very nearly the same. These matters are examined below.

EXPERIMENT

Single crystals of $\text{Fe}_{3-y}\text{Ti}_y\text{O}_4$ with $y < 0.05$ were grown from 99.999% Fe_2O_3 and 99.95% TiO_2 under a CO_2 atmosphere in a skull melter.^{21,22} The charge was maintained above its melting point for several hours; convective stirring optimized the uniform distribution of Ti^{4+} in the host. After cooling the boule, suitable single crystals were analyzed for titanium and iron composition by electron microprobe techniques. All precautions called for were properly observed, so as to optimize the uniformity of the Ti distribution. While the Ti content varied considerably with depth in the boule, the composition variable y tended to be quite uniform in the single crystals. Fifteen of these were selected and analyzed by microprobe techniques. Those with the most uniform Ti distribution were annealed as described below, cut to the appropriate geometry, and reanalyzed; these samples were more homogeneous in Ti content after the anneal than before. For the specimens used in the measurements the uncertainty in y remained in the range ± 0.0007 to ± 0.0009 , except for one sample with $y = 0.0206$ where the

uncertainty was ± 0.0016 .

Once the titanium-iron stoichiometry was known, the crystals were annealed under the appropriate CO-CO₂ buffer gas⁹ using a zirconia transfer cell²³ to monitor the oxygen fugacity. The ideal 4:3 oxygen to cation ratio was attained^{24,25} within 48 h at temperatures in the range 1200°C–1400°C. At higher temperatures annealing was more rapid, but upon quenching these specimens tended to shatter. Considerable difficulty was experienced in obtaining high-quality single crystals in the composition range $0.012 < y < 0.025$, where the titanium distribution tended to be nonuniform. Measurements were carried out on the best specimen for this composition range.

The crystals were trimmed with a diamond saw to remove outer layers of different composition produced during quenching, and cut into bars of approximately 2 mm × 2 mm × 10 mm. Four-probe leads were soldered ultrasonically and dc resistivity measurements were made from room temperature to liquid helium on both cooling and heating cycles.

RESULTS AND DISCUSSION

The resistivity data for Fe_{3-y}Ti_yO₄ are shown in Figs. 1 and 2 as plots of $\log \rho$ vs $1/T$ for the compositional ranges $0 \leq y \leq 0.0100$ and $0.0206 \leq y \leq 0.0380$, respectively. It is immediately evident that samples in these two ranges of y undergo a first- and a higher-order transition, respectively. No anomaly in electrical properties is encountered in the low-temperature range for titanomagnetites with $y > 0.0380$.²⁶

One should note that the plots in Figs. 1 and 2 are highly nonlinear and that the anomaly at T_V involves a semiconductor-semiconductor transition. Also, all data in the temperature range $T > T_V$ fall essentially on a universal curve, whereas for a fixed T in the range $T < T_V$ the resistivities assume steadily lower values as y is increased. Thus there is a significant spread in resis-

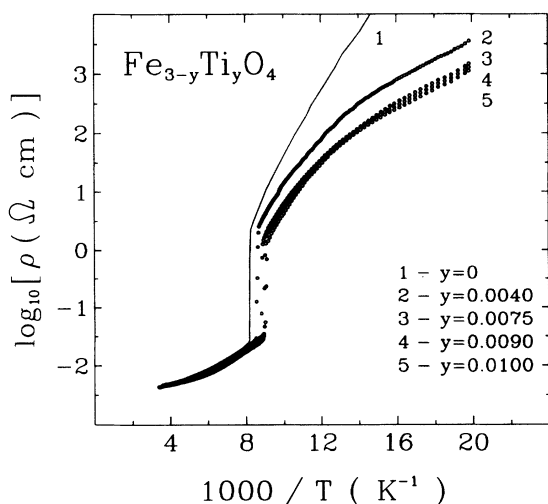


FIG. 1. Plot of $\log_{10}\rho$ vs $1/T$ for dilute titanomagnetites in the composition range of the first-order Verwey transition.

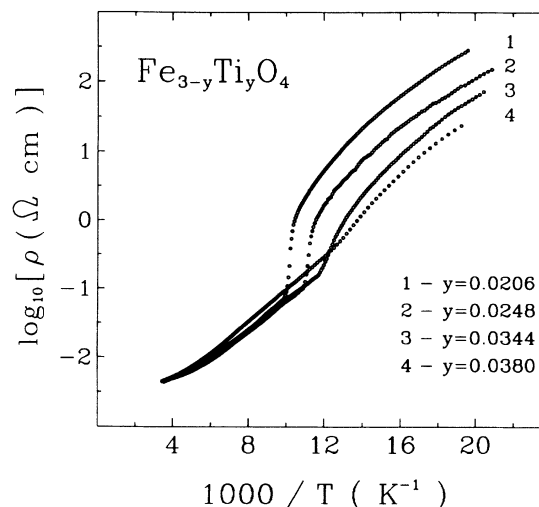


FIG. 2. Plot of $\log_{10}\rho$ vs $1/T$ for dilute titanomagnetites in the composition range of the higher-order Verwey transition.

tivity values below 120 K as the titanium content in magnetite is increased. Both T_V and the magnitude $\Delta\rho$ of the discontinuity diminish as y is increased. This latter trend is clearly displayed in Figs. 3 and 4, which show the smooth variation of $\Delta\rho$ with y . For samples undergoing the higher-order transition $\Delta\rho$ was computed from the region of the rapid change of ρ with T centered on T_V . In conformity with earlier practice,^{13,18} T_V was identified with the inflection point in the curves of Fig. 2.

There is a remarkable similarity of the present data with the electrical properties of Fe_{3(1-δ)}O₄ and of Fe_{3-x}Zn_xO₄ reported earlier.^{13,18} This is also illustrated in Figs. 3 and 4, which show a detailed comparison of the electrical properties of the titanomagnetites with nonstoichiometric magnetite in the vicinity of T_V . These

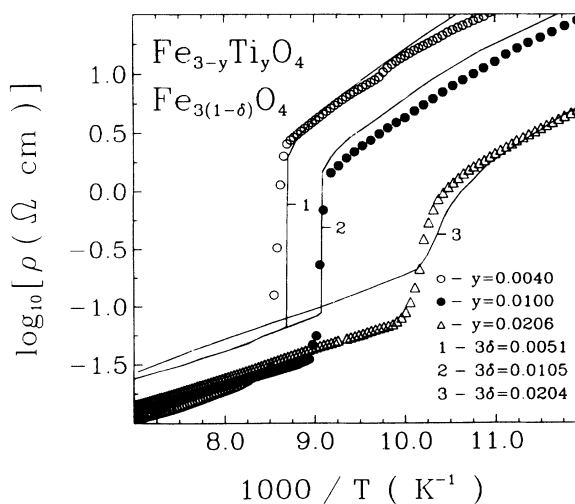


FIG. 3. Detailed comparison of electrical property of dilute titanomagnetites and nonstoichiometric magnetite near the Verwey transition; note the correspondence $y = 3\delta$.

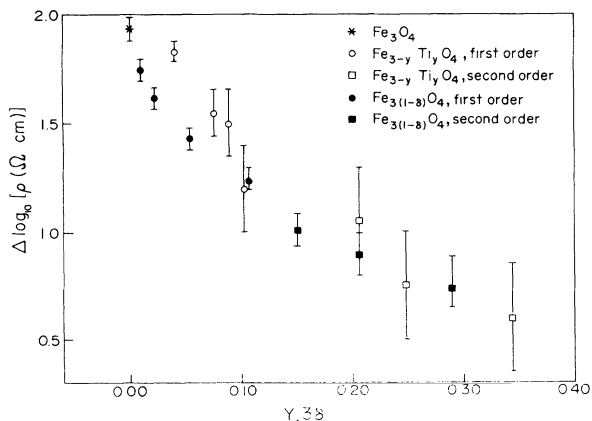


FIG. 4. Variation in the rapid change in resistivity near the Verwey transition, $\Delta \log_{10} \rho$ vs 3δ or y for nonstoichiometric magnetite or dilute titanomagnetite.

curves are representative of data for all other samples. It is evident that the correspondence $y = 3\delta$ applies to the variation of T_V with deviations from the parent composition Fe_3O_4 , just as the $x = 3\delta$ correspondence held for the zinc ferrite-nonstoichiometric magnetite system.¹⁸ Moreover, for $T < T_V$ the resistivity data for $\text{Fe}_{3(1-\delta)}\text{O}_4$ and for $\text{Fe}_{3-y}\text{Ti}_y\text{O}_4$ can be very nearly superposed. By contrast, the data for $T > T_V$ fall on two sets of very closely spaced curves. In this temperature range the resistivities of the various $\text{Fe}_{3(1-\delta)}\text{O}_4$ specimens are roughly half an order of magnitude larger than those of the $\text{Fe}_{3-y}\text{Ti}_y\text{O}_4$ samples. Similarly, for $T > T_V$ the resistivity curves of $\text{Fe}_{3(1-\delta)}\text{O}_4$ had been shown¹⁸ to lie somewhat above those of $\text{Fe}_{3-x}\text{Zn}_x\text{O}_4$. These findings are consistent with the elementary concept that the presence of cation vacancies is more deleterious to the electron transfer process than is the incorporation of Ti^{4+} ions, for which the radial extension of the orbitals is larger than that of the Fe^{3+} ions. Likewise, the incorporation of Zn^{2+} is far less damaging to electron transfer than the presence of vacancies.

Finally, we show in Fig. 5 a plot of the variation of T_V with x , y , and 3δ . The data for nonstoichiometric magnetite were read off from both heat capacity and resistivity measurements; heat capacity data are presently unavailable for the other systems. One clearly sees that data for all these systems superpose very well. Also, one can readily distinguish the first-order from the higher-order regimes. In both cases T_V changes linearly with sample composition; the ratio of the two slopes is $R \ln 2$, which fact can be rationalized by an elementary approach dealt with elsewhere.²⁷

A comparison of $\text{Fe}_{3-y}\text{Ti}_y\text{O}_4$ with the properties of

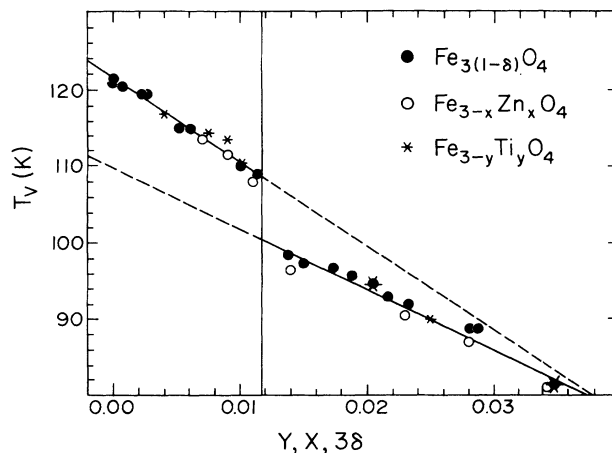


FIG. 5. Variation of Verwey transition temperature against sample composition for dilute titanomagnetite, zinc ferrite, or nonstoichiometric magnetite. The regions of first- and higher-order transitions are clearly delineated.

$\text{Fe}_{3-x}\text{Zn}_x\text{O}_4$ reported earlier¹⁸ shows that in the range $0 \leq x, y \leq 0.04$ both systems display very similar electrical characteristics. In zeroth order the mirror symmetry referred to in the Introduction is satisfied. One should note that iron on the tetrahedral sites is exclusively in the trivalent state for nonstoichiometric (vacancy-containing) magnetite, zinc ferrites, and titanomagnetites, in the dilute concentration range; this fact has been established by appropriate saturation magnetization studies.²⁸ The striking electrical similarities of all three classes of materials derived from the parent Fe_3O_4 suggest that conduction occurs via charge fluctuations among the cations in octahedral interstices without involving (Fe^{3+}) on tetrahedral sites. The "mirror-image" properties further suggest that charge transport likely involves small polarons as carriers, since in such a regime $\sigma \sim cv \approx c(1-c)$, where c is the charge carrier density.

In conclusion, we have shown that the electrical properties of $\text{Fe}_{3(1-\delta)}\text{O}_4$, $\text{Fe}_{3-x}\text{Zn}_x\text{O}_4$, and $\text{Fe}_{3-y}\text{Ti}_y\text{O}_4$ are very similar in their dependence on 3δ , x , or y , and in their variation with temperature. These findings are consistent with charge transport by thermal activation involving charge fluctuations among ferrous and ferric ions on octahedrally coordinated interstices.

ACKNOWLEDGMENTS

This research was supported by NSF Grant No. DMR 89-21293. Additional support for J. Stickler through NSF Grant No. DMR 89-05605 is also acknowledged.

*Permanent address: Akademia Górniczo-Hutnicza, Kraków, Poland.

†Permanent address: Department of Chemistry, Ohio Northern University, Ada, OH 45810-1599.

‡Permanent address: Division of Mathematics, Science & Technology, Valley City State University, Valley City, ND 58072.

¹E. J. W. Verwey, *Nature (London)* **144**, 327 (1939).

²E. J. W. Verwey and R. W. Haayman, *Physica (Utrecht)* **8**, 979

- (1941).
- ³C. A. Domenicali, *Phys. Rev.* **78**, 458 (1950).
- ⁴B. A. Calhoun, *Phys. Rev.* **94**, 1577 (1954).
- ⁵A. J. M. Kuipers and V. A. M. Brabers, *Phys. Rev. B* **14**, 1401 (1976).
- ⁶A. J. M. Kuipers and V. A. M. Brabers, *Phys. Rev. B* **20**, 594 (1979).
- ⁷B. Gillot and F. Jemmali, *Phys. Status Solidi A* **77**, 339 (1983).
- ⁸S. Iida, *Philos. Mag. B* **24**, 349 (1980).
- ⁹R. Aragón, D. J. Buttrey, J. P. Shepherd, and J. M. Honig, *Phys. Rev. B* **31**, 430 (1985).
- ¹⁰R. Aragón, J. P. Shepherd, J. W. Koenitzer, D. J. Buttrey, and J. M. Honig, *J. Appl. Phys.* **57**, 3221 (1985).
- ¹¹J. P. Shepherd, J. W. Koenitzer, R. Aragón, C. J. Sandberg, and J. M. Honig, *Phys. Rev. B* **31**, 1107 (1985).
- ¹²J. P. Shepherd, R. Aragón, J. W. Koenitzer, and J. M. Honig, *Phys. Rev. B* **32**, 1818 (1985).
- ¹³R. Aragón, R. J. Rasmussen, J. P. Shepherd, J. W. Koenitzer, and J. M. Honig, *J. Magn. Mater.* **54–57**, 1335 (1986).
- ¹⁴G. Haley, J. G. Mullen, and J. M. Honig, *Solid State Commun.* **69**, 285 (1989).
- ¹⁵Z. Kaçol, R. N. Pribble, and J. M. Honig, *Solid State Commun.* **69**, 793 (1989).
- ¹⁶Z. Kaçol and J. M. Honig, *Solid State Commun.* **70**, 967 (1989).
- ¹⁷Z. Kaçol and J. M. Honig, *Phys. Rev. B* **40**, 9090 (1989).
- ¹⁸P. W. Wang, Z. Kaçol, M. Wittenauer, and J. M. Honig, *Phys. Rev. B* **42**, 4553 (1990).
- ¹⁹J. P. Shepherd, J. W. Koenitzer, R. Aragón, J. Spažek, and J. M. Honig, *Phys. Rev. B* **43**, 8461 (1991).
- ²⁰J. M. Honig, *J. Chem. Ed.* **43**, 76 (1966).
- ²¹H. R. Harrison and R. Aragón, *Mater. Res. Bull.* **13**, 1097 (1978).
- ²²R. Aragón, H. R. Harrison, R. H. McCallister, and C. J. Sandberg, *J. Cryst. Growth* **61**, 221 (1983).
- ²³J. P. Shepherd and C. J. Sandberg, *Rev. Sci. Instrum.* **55**, 1696 (1984).
- ²⁴R. Aragón and R. H. McCallister, *Phys. Chem. Minerals* **8**, 112 (1982).
- ²⁵J. M. Honig and R. Aragón, *Z. Anorg. Allg. Chem.* **540/541**, 80 (1986).
- ²⁶R. Rasmussen, Ph.D. thesis, Purdue University, 1988.
- ²⁷J. M. Honig, *Phys. Chem. Minerals* **15**, 476 (1988).
- ²⁸Z. Kaçol, J. Sabol, and J. M. Honig, *Phys. Rev. B* **43**, 649 (1991).